Vacuum 164 (2019) 62–65

Contents lists available at ScienceDirect

Vacuum

journal homepage: www.elsevier.com/locate/vacuum

Short communication

High-density and low-interstitial Ti-23Al-17Nb prepared by vacuum pressureless sintering from blended elemental powders

Haiying Wang[a], Ce Zhang[a], Fang Yang[a,*], Peng Cao[b,d], Zhimeng Guo[a,**], Boxin Lu[a], Cunguang Chen[a], Peng Liu[b], Alex A. Volinsky[c]

[a] Institute for Advanced Materials& Technology, University of Science and Technology Beijing, Beijing, 100083, China
[b] Department of Chemical and Materials Engineering, University of Auckland, Private Bag 92019, Auckland, 1142, New Zealand
[c] Department of Mechanical Engineering, University of South Florida, Tampa, FL, 33620, USA
[d] MacDiarmid Institute for Advanced Materials and Nanotechnology, PO Box 600, Wellington, 6140, New Zealand

ARTICLE INFO

Keywords:
Ti_2AlNb alloy
Blended elemental powder
Vacuum sintering
Microstructure
Mechanical property

ABSTRACT

High-quality Ti_2AlNb alloys were prepared from blended elemental powders via cold isostatic pressing and pressureless vacuum sintering. When sintered at 1200 °C, the Ti-23Al-17Nb alloy attained a very high relative density (98.7%) and low contents of interstitials (0.1 wt% O, 0.03 wt% N and 0.005 wt% H). Three crystalline phases – B2, α_2, and orthorhombic (O) – were observed in a fine and homogeneous microstructure in the sintered samples. The fine microstructure and low interstitials account for the good mechanical properties achieved: approximately 941 MPa of ultimate tensile strength, 862 MPa of yield strength and 11.7% of elongation.

Ti_2AlNb alloys based upon the orthorhombic (O) phase have gained significant attention for use in the aerospace and military industries in the past decades due to their high specific strength and good high-temperature properties [1–3]. However, Ti_2AlNb alloys have yet found widespread applications, compared to traditional Ni-based superalloys due to their high processing costs. Powder metallurgy (PM) has long been regarded as a promising method to reduce the processing costs owing to its near-net-shape capability. In general, fine and homogenous microstructures can be achieved by PM routes. Two representative processing routes are commonly used, either from pre-alloyed (PA) powder or blended elemental (BE) powder. The Ti_2AlNb PA powder produced by atomization is perfectly spherical with a mean particle size ranging from 40 to 80 μm. The coarse spherical powder causes the poor sinterability due to their small specific surface area. Therefore, hot isostatic pressing (HIP) [4], hot pressing (HP) [5] and spark plasma sintering (SPS) [6] are commonly required to densify the compacts made of PA powder. Another way to produce Ti_2AlNb alloys is through densification of elemental Ti and Al, and prealloyed Al-Nb powders. However, the Ti2AlNb alloys made by BE method sometimes have unsatisfactory sintered density and excessive interstitial contents. For Ti_2AlNb and TiAl alloys, the interstitial oxygen should be strictly controlled under 0.1 wt% [7], beyond which the ductility and hot-workability will be significantly reduced. Low sintered density is also a major issue if the BE compacts are sintered by pressureless vacuum sintering method, due to the well-known Kirkendall effect between Ti and Al. To achieve high sintered density, hot pressing [8] and SPS [9] are often used. In our previous work, fully dense Ti-6Al-4V [10] and Ti-TiC composites [11] were successfully fabricated by vacuum pressureless sintering. The O content in the as-sintered materials was below 2000 ppm, and the N content was below 500 ppm. Good mechanical properties, in particular high ductility, were obtained in the sintered samples. This paper reports that a nearly full-density Ti-23Al-17Nb alloy was produced from BE powder compacts, with low interstitials and good mechanical properties.

The TiH_2 powder (particle size: 180–830 μm), Nb-25.9 wt%Al master alloy (0.5–7 mm) and Al powder (D_{50} = 4.8 μm) were selected as the raw materials. First, the TiH_2 and Nb-Al powders were crushed by vibratory milling under vacuum respectively. Only fine powders (D_{50} < 10 μm) were used for the subsequent powder compaction. The fine TiH_2, Nb-Al and Al powders with a mass ratio of 100:71:6 were blended in a mixer under Ar atmosphere for 2 h. The blended powders were then subjected to a pre-treatment in a vacuum rotary furnace at 700 °C for 5 h. This pre-treatment resulted, in the interdiffusion between Al and Ti, and dehydrogenation of TiH_2 simultaneously. After another crushing process, the powder mixture was compacted by cold isostatic pressing (CIP) at 200 MPa. The compacts were then sintered at

* Corresponding author.
** Corresponding author.
E-mail addresses: yangfang@ustb.edu.cn (F. Yang), zmguo@ustb.edu.cn (Z. Guo).

https://doi.org/10.1016/j.vacuum.2019.03.001
Received 16 December 2018; Received in revised form 28 February 2019; Accepted 1 March 2019
Available online 06 March 2019

Table 1
Relative density and chemical composition (wt.%) of different samples.

Sample	Relative density %	Ti	Nb	Al	H	O	N
T 1100 °C	95.1 ± 0.5	Bal.	30.75	14.21	0.01	0.09	0.034
T 1150 °C	96.3 ± 0.5	Bal.	30.56	14.02	0.007	0.11	0.028
T 1200 °C	98.7 ± 0.3	Bal.	31.21	13.97	0.005	0.1	0.03
T 1200 °C/HIP	99.5 ± 0.3	Bal.	30.67	14.38	0.003	0.12	0.032

1100, 1150 and 1200 °C for 5 h with a heating rate 2 °C/min under vacuum of 10^{-3} Pa. Finally, hot isostatic pressing (HIP) was performed on the samples sintered at 1200 °C (Sample T1200 °C in Table 1) to obtain full density. The HIP parameters were 1000 °C/100 MPa/2 h. In the entire procedure, powder transfer and powder handing were undertaken in the sealed container or glovebox under Ar atmosphere to avoid interstitials pick-up.

Particle size distribution of the powder was measured by laser particle size distribution instrument (BT-9300S). The O content of the samples was measured by non-dispersive infrared analysis, and the N/H contents were determined by the thermal conductivity method, with an Eltra ONH-2000 apparatus. Al and Nb contents were determined by titration. The phase constituents of the blend elemental powder and pre-treated powder were analyzed by X-ray diffraction (XRD, Shimadzu XRD-6000, Cu Kα target, 40 kV and 40 mA, 2θ = 20°–80°). Room temperature tensile tests were conducted at an initial strain rate of 1×10^{-3} s^{-1} on an AGI-250KN machine. The as-sintered microstructures and powder morphology were analyzed by optical microscopy (OM, Axio Imager M2m) and scanning electron microscopy (SEM, Philips LEO-1450) equipped with energy-dispersive spectroscopy (EDS).

Fig. 1(a) shows the morphology of the blend elemental powder, including TiH_2, Nb-Al master alloy powder with irregular shape and spherical Al powder. It is known that diffusion coefficient of Al in Ti is much greater than that of Ti in Al [12]. As a result, the well-known Kirkendall effect leads to the micropores in the sintered Ti-Al compacts. The number of the Kirkendall pores increases with the amount of Al powder. It is therefore technically very difficult to achieve fully dense alloys from the blended elemental powder.

In this work, we proposed a pre-treatment to mitigate the adverse Kirkendall effect. The XRD patterns of the BE powder, pre-treated powder and as-sintered materials are shown in Fig. 1(c). It is clear that TiH_2 and Al peaks were detected in the BE powder. The diffraction peaks at 25.4°, 38.9° and 37.5°, 41.4° correspond to the (101), (112) planes of Al_3Nb phase and the (410), (411) of $AlNb_2$ phase in the Nb-Al master alloy powder. After pre-treatment process, α-Ti phase emerges because of dehydrogenation. More prominent is the disappearance of Al peaks, indicating that Al has completely diffused to Ti. The diffusion between Nb-Al master alloy particles and Ti particles cannot be excluded. It is noted that not orthorhombic Ti_2AlNb phase (as known as O phase) was detected in the pre-treated powder. The lack of the O phase implies the low diffusion rate of Nb at low temperatures. It is known that the diffusion coefficient of Nb is lower than Ti and Al by a factor of 2–3 in binary Ti-Al compounds [13]. We proposed the reaction and phase transformation sequences in the pre-treatment process as:

$$TiH_2 \rightarrow Ti + H_2 \quad (1)$$

$$Ti + Al \rightarrow TiAl_3 \quad (2)$$

$$Ti + Al_3Nb \rightarrow AlNb_2 + TiAl_3 \rightarrow AlNb_3 + TiAl_3 \quad (3)$$

The morphology of the pre-treated powder after crushing is shown in Fig. 1(b). The particle size distribution analysis shows results of D_{10} = 2.15 μm, D_{50} = 6.49 μm, D_{90} = 13.05 μm. The use of fine powder particles is beneficial for the as-sintered density, as shown in Table 1. A relative sintered density of > 95.1%, was observed in these sintered compacts. The change in quantity and shape of residual pores in the matrix further confirms the achievement of high density. As reported in the previous studies, high-density Ti_2AlNb alloys can only obtained by pressureless sintering at a high temperature > 1300 °C [14], or with assistance of high pressure such as HIP at > 100 MPa [4,15], or electric field such as SPS [5,6,8,9]. We believe the partial-alloying and cleansing effect of TiH_2 dehydrogenation [16,17] during the pre-treatment promote the densification process. Moreover, the partial alloying process eliminates the possible swelling effect arising from the un-balanced Kirkendall diffusion. In addition to the cleansing effect of dehydrogenation, we used either high vacuum or argon atmosphere for the powder handling; therefore the contamination has been minimized. In our previous study, the powder with D_{50} = 11 μm had a high oxygen content of 0.46–0.49 wt% when exposed to the air [11]. In contrast, the O content of the as-sintered samples was controlled to 0.09–0.12 wt%, and the N content was about 0.028–0.034 wt % (Table 1).

For the samples sintered at low temperatures, some compositional inhomogeneity was observed. For example, in sample T1100 °C, some Nb-rich particles are visible and EDS analysis show compositions of 41.7 wt% Nb and 16.2 wt% Al (Fig. 2). By increasing temperature, elements Nb and Al completely diffuse to Ti, resulting in homogeneous microstructures, as shown in Fig. 2(b and c). When the samples were sintered at high temperatures, e.g. at 1150 °C or 1200 °C, the O phase grew into coarse lamellar morphology from short lath and α_2 also grew larger. AT these high temperatures (i.e., in single B2 phase field for Ti-23Al-17Nb), not only the compositional homogeneity has been achieved, but also the residual pores almost diminished. As shown in Fig. 2(c), a few integrated B2 grains can be observed in the matrix. Upon furnace cooling, the α_2 nuclei firstly initiate to form at the B2 grain boundary and grow to large α_2-rich grains [18]. Meanwhile, the O phase precipitates in the interior of B2 grains and grow to long and coarse O + B2 lamellar microstructure. There are two types of O phase: primary O phase with residual B2 to form a coarse lath shape, and secondary O phase with an ultrafine acicular shape precipitated in residual B2 by phase transformation of B2 → B2 + O [6]. If the sintered sample undergoes a further HIP treatment at 1000 °C (sample T1200 °C/HIP), phase transformations of O → α_2 + B2 and α_2 + O + B2 → α_2 + B2 occur in sequence during the heating process.

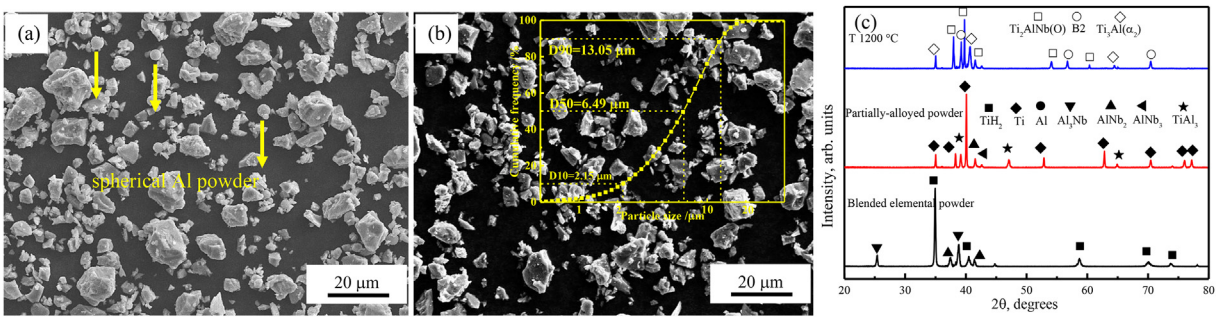

Fig. 1. SEM images of blended elemental powder(a), partially-alloyed powder (b) and XRD patterns of the powders and as-sintered materials (c).

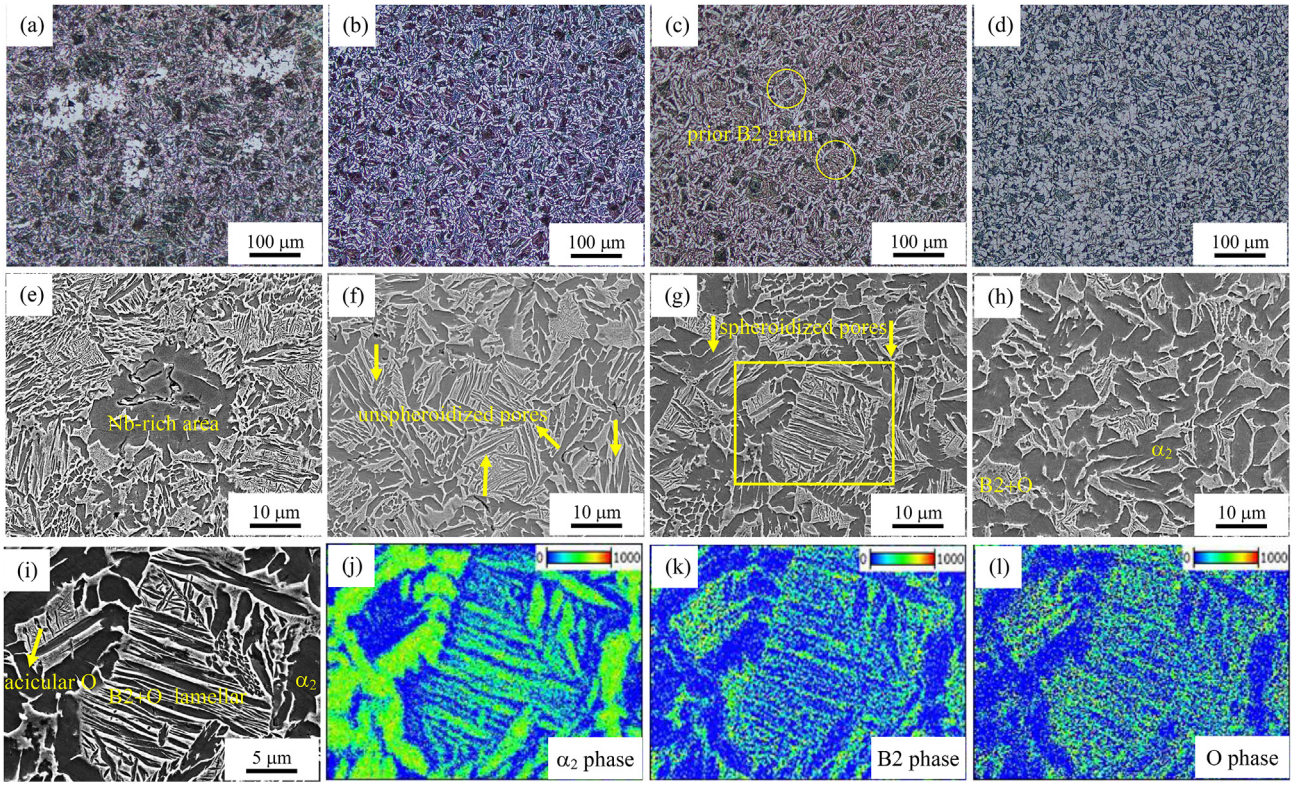

Fig. 2. OM and SEM micrographs of the different as-sintered Ti-23Al-17Nb samples: (a, e) T 1100 °C; (b, f) T 1150 °C; (c, g) T 1200 °C. and (d, h) T 1200 °C/HIP, and FESEM mapping taken from yellow box in Fig. 3(g): (i–l). (For interpretation of the references to colour in this figure legend, the reader is referred to the Web version of this article.)

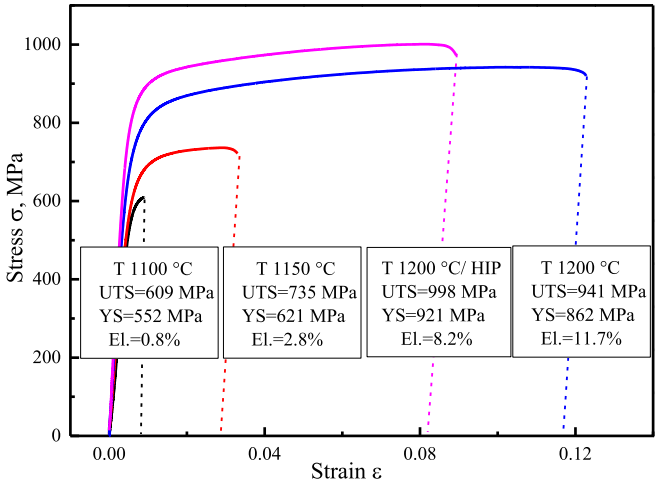

Fig. 3. Stress strain curves of the as-sintered Ti-23Al-17Nb alloys.

The dissolution of the O phase, growth and aggregation of α_2 phase take place, resulting in large amount of granular α_2 along the B2 grain boundary [19].

Representative engineering stress-strain curves are presented in Fig. 3. It is clear that ultimate tensile strength (UTS) and yield strength (YS) increase with sintering temperature: from 609 MPa to 998 MPa for UTS and 552 MPa–921 MPa for YS. The strength increase mainly stems from the higher sintering density. It is generally agreed that a relative density over 98% would give rise to a similar strength to the wrought alloys. The elongation of sample T1200 °C is about 11.7%, much higher than that reported in other similar alloys sintered from BE powder (< 5%) [8,20]. We believe the improved ductility is due to the low interstitial concentration. It was worth noting that the T1200 °C sample still had a few residual pores, although it had a high sintered density. Therefore, non-capsule HIP was employed to further improve the density. The T1200 °C/HIP sample had a slightly higher strength yet reduced ductility. The reduction in ductility after HIP may be due to the formation of more brittle α_2 phase.

In conclusion, a partial-alloying pre-treatment method was successfully developed and integrated into the conventional blended elemental powder sintering process. Nearly full density was achieved in Ti_2AlNb alloy by pressureless sintering. The samples demonstrated homogeneous microstructures and low interstitial content. Consequently, good mechanical properties were achieved in the sintered Ti_2AlNb alloy with 941 MPa of UTS, 862 MPa of YS and 11.7% of elongation.

Acknowledgment

This work was supported by China Postdoctoral Science Foundation (No. 2018M641188) and the State Key Lab for Advanced Metals and Materials (No. 2016-ZD02).

References

[1] D. Banerjee, A.K. Gogia, T.K. Nandy, A new ordered orthorhombic phase in a Ti_3Al–Nb alloy, Acta Metall. 36 (1988) 871–882.
[2] S. Emura, K. Tsuzak, K. Tsuchiya, Improvement of room temperature ductility for Mo and Fe modified Ti_2AlNb alloy, Mater. Sci. Eng., A 528 (2010) 355–362.
[3] K. Muraleedharan, T.K. Nandy, D. Banerjee, Phase stability and ordering behaviour of the O phase in Ti–Al–Nb alloys, Intermetallics 3 (1995) 187–199.
[4] J. Wu, L. Xu, Z. Lu, Microstructure design and heat response of powder metallurgy Ti_2AlNb alloys, J. Mater. Sci. Technol. 31 (2015) 1251–1257.
[5] J. Jia, K. Zhang, S. Jiang, Microstructure and mechanical properties of Ti–22Al–25Nb alloy fabricated by vacuum hot pressing sintering, Mater. Sci. Eng., A 616 (2014) 93–98.
[6] K.H. Sim, G. Wang, Y.M. Li, Enhanced ductility of a bimodal grain structure Ti–22Al–25Nb alloy fabricated by spark plasma sintering, Adv. Eng. Mater. 19

(2017) 1600804.
[7] P.R. Smith, A.H. Rosenberger, M.J. Shepard, Review a P/M approach for the fabrication of an orthorhombic titanium aluminide for MMC applications, J. Mater. Sci. 35 (2000) 3169–3179.
[8] G. Wang, J. Yang, X. Jiao, Microstructure and mechanical properties of Ti–22Al–25Nb alloy fabricated by elemental powder metallurgy, Mater. Sci. Eng., A 654 (2016) 69–76.
[9] K.H. Sim, G. Wang, J. Ju, Microstructure and mechanical properties of a Ti − 22Al − 25Nb alloy fabricated from elemental powders by mechanical alloying and spark plasma sintering, J. Alloy. Comp. 704 (2017) 425–433.
[10] C. Zhang, B. Lu, H. Wang, Vacuum pressure-less sintering of Ti − 6Al − 4V alloy with full densification and forged-like mechanical properties, J. Mater. Eng. Perform. 27 (2018) 282–292.
[11] C. Zhang, Z. Guo, F. Yang, In situ formation of low interstitials Ti − TiC composites by gas-solid reaction, J. Alloy. Comp. 769 (2018) 37–44.
[12] Y. Mishin, C. Herzig, Diffusion in the Ti–Al system, Acta Mater. 48 (2000) 589–623.
[13] S. Divinski, F. Hisker, C. Klinkenberg, Niobium and titanium diffusion in the high niobium-containing Ti–54Al–10Nb alloy, Intermetallics 14 (2006) 792–799.
[14] T.K. Lee, E.I. Mosunov, S.K. Hwang, Consolidation of a gamma TiAl–Mn–Mo alloy by elemental powder metallurgy, Mater. Sci. Eng., A 239–240 (1997) 540–545.
[15] C.F. Yolton, J.P. Beckman, Powder metallurgy processing and properties of the ordered orthorhombic alloy Ti-22at.%Al-23at.%Nb, Mater. Sci. Eng. A 192–193 (1995) 597–603.
[16] G. Chen, P. Cao, N. Edmonds, Porous NiTi alloys produced by press-and-sinter from Ni/Ti and Ni/TiH_2 mixtures, Mater. Sci. Eng., A 582 (2013) 117–125.
[17] G. Chen, P. Cao, NiTi powder sintering from TiH_2 powder: an in situ investigation, Metall. Mater. Trans. 44 (2013) 5630–5633.
[18] C.J. Boehlert, B.S. Majumdar, V. Eetharaman, Part I. The microstructural evolution in Ti-Al-Nb O + Bcc orthorhombic alloys, Metall. Trans. A 30 (1999) 2305–2323.
[19] B. Shao, Y. Zong, D. Wen, Investigation of the phase transformations in Ti − 22Al − 25Nb alloy, Mater. Char. 114 (2016) 75–78.
[20] Y.J. Cheng, S.Q. Li, X.B. Liang, Effect of deformed microstructure on mechanical properties of Ti–22Al–25Nb alloy, Trans. Nonferrous Metals Soc. China 16 (2006) s2058–s2061.